Correlation between saturated fatty acid chain-length and intermolecular forces determined with terahertz spectroscopy

Shuting Fan,[a] Michael T. Ruggiero,[b] Zhengfang Qian*[a] and Vincent P. Wallace†[c]

[a] College of Electronic Science and Technology, Shenzhen University, 3688 Nanhai Rd, Shenzhen, Guangdong Province, China, 518060.
[b] Department of Chemistry, University of Vermont, 82 University Place, Burlington, Vermont, 05405, United States of America.
[c] Department of Physics, The University of Western Australia, 35 Stirling Highway, Perth, WA, 6009, Australia.

* zq001@szu.edu.cn
† vincent.wallace@uwa.edu.au

We measured crystalline (C-form) saturated fatty acids with even carbon numbers ranging from 12 to 20 using temperature dependent terahertz time-domain spectroscopy (THz-TDS). Absorption features between 0.5 to 2.75 THz were identified at temperatures from 96 K to 293 K, and a systematic red-shift was obvserved with the increasing carbon chain length. The origins of these absorption bands were uncovered using state-of-the-art *ab initio* density functional theory (DFT) calculations. Similar vibrational motions in the absorption bands of the different materials highlight the unique role that THz-TDS has for probing weak non-covalent interactions in these materials. Our results showcase the utility of the terahertz region, which is beyond the scope of related vibrational techniques, providing direct evidence of the effect of chain length on the intermolecular interactions of these molecules.

Fatty acids are an important class of biomolecules consisting of a non-polar aliphatic hydrocarbon chain terminated by a carboxylic acid head group. Naturally occurring fatty acids often contain an even number of carbon atoms, are unbranched, and play a critical role in countless biological processes. While many recognize fatty acids as a fuel source, they also contribute significantly to the proper functioning of cellular processes. For instance, free fatty acids (FFA), together with cholesterol, ceramides, and dead corneocytes, form a rigid 'brick and mortar' structured stratum corneum (SC) layer in mammalian epidermises whose barrier function is essential to mammal survival [1, 2]. It is well known that the carbon chain length of the fatty acid molecules is closely associated with their functionalities, and often abnormalities in their structure are a sign of serious pathological disease. A study in 2014 found that the FFAs present in the SC layer of patients suffering from atopic eczema (AE) have a shorter chain length on average compared to those from the healthy control group or from the non-lesioned skin of the AE patients [3]. The reduction in carbon chain length of the epidermal surface lipids results in a less ordered hexagonal lateral packing of the lipids and disrupts the barrier function of the SC layer in AE patients. In contrast, the longer carbon chains can form a denser and highly ordered orthorhombic organization that maintains the functionality of the SC layer in healthy people. The differences in the chain length of the FFAs could also cause opposite metabolic consequences when ingested. Palmitic acid (C16:0) uptake can increase low-density lipoprotein (LDL) cholesterol level as well as atherosclerosis risks, whereas stearic acid has the exact opposite effect [4]. Clearly, the structures and associated intermolecular interactions in various FFAs plays a significant role on physiological behaviour, and additionally these phenomena are of great importance in other fields, such as the pharmaceutical, cosmetics, and food industries [5]. Thus, an in-depth investigation into the three-dimensional packing and associated intermolecular forces in biologically-relevant FFAs is critical to understand and predict the behaviour of this important class of materials.

Crystalline FFAs offer an efficient means of probing the forces present with atomic-level precision. While clearly the crystalline form is often not directly used *in vivo*, the arrangement of fatty acids in materials like cell membranes represents a pseudo-ordered material, with a bulk arrangement that closely resembles what is found in the crystal [6, 7]. The molecular assembly of fatty acids has previously been studied using several methods. Both Fourier transform infrared spectroscopy (FTIR) and Raman spectroscopy have been used to investigate the vibrational dynamics of these materials [8, 9, 10, 11]. However, these mid-IR methods probe the high frequency vibrational modes (above 200 cm^{-1}), which are primarily associated with intramolecular interactions such as the deformation of covalent bonds. While these methods are powerful for understanding the nature of the intramolecular forces, they only provide indirect information into the intermolecular forces, and therefore the molecular packing and related phenomena.

Recently, THz-TDS has been proven to be a powerful tool for probing the intermolecular forces in molecular solids. Terahertz, or far-IR, radiation (~0.3-10 THz or ~10-333 cm^{-1}) can excite low-frequency large-amplitude collective vibrational motions in condensed phase materials, which subsequently probe a large portion of both the intermolecular and intramolecular potential energy hypersurface. While conceptually similar to the more common FTIR spectroscopy, the nature of terahertz motions are shaped by long-range interactions, which results in each material having a unique spectral fingerprint at terahertz frequencies. This has led to THz-TDS being used to investigate many condensed phase materials, including polymorphism of crystal structures [12, 13, 14], protein and water dynamics [15, 16], and phase transformation phenomena [17, 18]. The intermolecular vibrational modes of many biologically

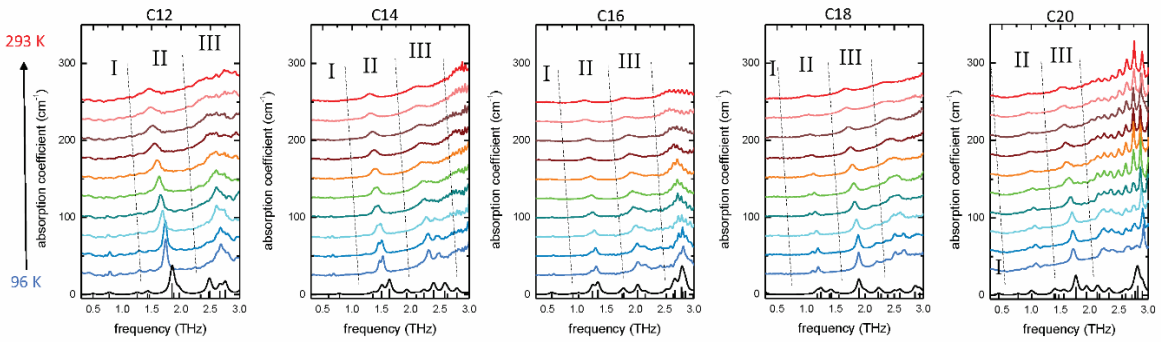

Fig. 1 The temperature dependent terahertz spectra of the fatty acids measured. The curves in colour are the absorption coefficients calculated from the experiment. The black curves are the simulated vibrational spectra from our DFT calculations.

important materials, such as amino acids [19, 20], short chain peptides [21], nucleobases and the corresponding nucleosides [22], have been successfully probed with THz-TDS.

The dependence of terahertz phonons on the entire potential energy hypersurface has a serious consequence, in that even in materials where the molecular conformations are identical but where the bulk arrangements differ (i.e. polymorphism), the two spectra cannot be directly compared. Unlike the mid-IR, where specific motions are known to occur at predictable frequencies and a large set of materials can be screened by observing spectral 'shifting', the terahertz motions in different materials are far too complex, and often very different, to make direct comparisons possible. However, in the case of the naturally occurring crystalline FFAs, the packing motifs, symmetry, and overall forces are all consistent, making them one of the few cases where spectral changes across the series can be identified, quantified, and explored in detail using THz-TDS. Five saturated FFAs with even carbon numbers were acquired from Sigma-Aldrich, namely lauric acid (C12), myristic acid (C14), palmitic acid (C16), stearic acid (C18), and arachidic acid (C20). These samples were used without further purification. We prepared the samples by depositing molten FFA onto a z-cut quartz window, followed by placing a second quartz window on top prior to solidification and recrystallization. The samples were measured in a commercial THz-TDS system (Terapulse4000, TeraView, Ltd., Cambridge, UK). The details on the terahertz measurements are available in the ESI. All samples were confirmed to be in the C form by powder X-ray diffraction experiments.

The temperature dependent terahertz spectra of the measured fatty acids are shown in Fig. 1. Due to spectral bandwidth limitations, our analysis is restricted to frequencies below 2.75 THz, where it was observed that the absorption features were concentrated in three frequency bands labelled I, II, III in Fig. 1. As the temperature was increased from 96 K to 293 K, the features undergo a red-shift, which is attributed to the thermal expansion of the crystalline lattice [23]. Band I exhibits very weak absorption peaks at low frequencies that are buried in the thermal noise as the temperature increases. The broad feature in band II at 293 K becomes much more prominent at lower temperatures for lauric acid and arachidic acid, while it at the same time splits into two closely located peaks in that of myristic acid, palmitic acid and stearic acid.

Interestingly, apart from the temperature dependent shift, a chain length dependent pattern is also identified from our experiment. At 96 K, the absorption bands evolve to lower frequencies with the lengthening of the carbon chain as shown in Fig. 2. Moreover, when the multiple features in each band evolve into one single broad peak at 293 K, the dependence of the peak locations to the carbon atom number becomes linear as plotted in Fig. 3. While, in general, materials with different compositions cannot reasonably have their terahertz spectra readily compared (i.e. comparing spectral shifting) due to the dependence of terahertz transitions on the entire potential energy surface, this class of materials are all isostructural, implying that in this particular case spectral shifting can be interpreted meaningfully. However, unlike more traditional mid-IR methods, the lack of functional group specific transitions at terahertz frequencies necessitates the use of advanced computational methods in order to interpret and assign low-frequency spectral data.

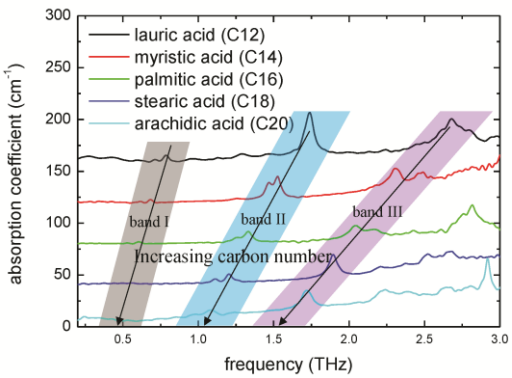

Fig. 2 The evolving of the absorption bands with increasing carbon atom number at 96 K.

Table 1 Experimental and simulated vibrational transitions for the peaks in bands I, II, and III, as well as the vibrational force constants and reduced masses .

Carbon number	Band I				Band II				Band III			
	Peak position (THz)		Force constant (N/m)	Reduced Mass (AMU)	Peak position (THz)		Force constant (N/m)	Reduced Mass (AMU)	Peak position (THz)		Force constant (N/m)	Reduced Mass (AMU)
	Exp. (96K)	Sim.			Exp. (96K)	Sim.			Exp. (96K)	Sim.		
12	0.79	0.7752	0.2127	5.4069	1.74	1.8474	0.9755	4.3660	2.68	2.4702	1.6781	4.2007
14	0.68	0.7840	0.2141	5.3208	1.53	1.6381	0.7935	4.5166	2.31	2.3906	1.6395	4.3819
16	0.61	0.5763	0.0944	4.3408	1.26	1.2684	0.5102	4.8439	2.04	2.0391	1.1205	4.1164
18	-	0.2820	0.0231	4.4379	1.11	1.1850	0.4309	4.6874	1.90	1.8986	1.0496	4.4478
20	-	0.1383	0.0055	4.3984	1.08	1.0097	0.3144	4.7105	1.72	1.7621	0.9025	4.4396

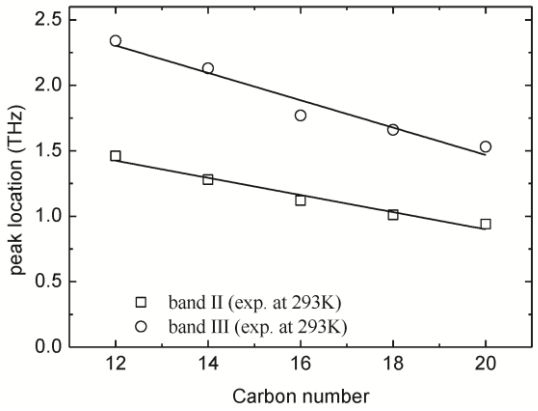

Fig. 3 The linear dependence of the peak location on the carbon number at 293 K. Band I is buried in the thermal noise

Fully-periodic density functional theory (DFT) simulations were performed using the CRYSTAL17 software package [24]. The 6-311g (2d, 2p) basis set [25] and Perdew-Burke-Ernzerhof (PBE) [26] density functional were used in conjunction with the D3-BJ dispersion correction by Grimme *et al* [27, 28]. The geometries of each crystal were fully optimized with no constraints other than translational and space group symmetry (lattice vectors and atomic positions free to relax), and upon complete optimization the vibrational normal modes and frequencies were determined using a finite-difference method, with IR-intensities calculated using the Berry Phase method [29, 30, 31]. The results of the vibrational simulations are also shown at the bottom of Fig. 1, and are in excellent agreement with the experimentally observed spectra.

Analysis of the individual vibrational modes in the studied materials highlights that there indeed do exist identical mode-types that persist throughout increasing chain length. Additionally, there is an increasing vibrational density of states with increasing chain length, which is expected given the number of vibrations in solids scales linearly with the number of atoms within a given unit cell. All of the vibrations in the highlighted regions correspond to large-amplitude motions of the carbon tails about the central carboxylate head (videos of the representative motions are available in the ESI). The prominent feature in band I corresponds to a rigid rotation of the carbon chain, with two chains joined via hydrogen bonds moving symmetrically. The main features in bands II and III correspond to a torsion of the carbon chain about the centre of the chain, with II corresponding to in-phase motion between adjacent molecules while III corresponds to out-of-phase motion.

The assignment of the experimental spectra using the DFT simulations enables a more in-depth description of the intermolecular forces present in these materials to be obtained. Based on the solution of the vibrational Schrodinger equation, the frequencies of vibrational transitions are dependent on both the reduced mass and the force constant for a given mode. Decomposition of these parameters for specific vibrational modes in the studied fatty acid crystals (Table 1) highlights that while the reduced masses generally decrease with increasing chain length (which would result in a larger vibrational transition energy), the force constants drastically decrease with increasing chain length. Thus, the origins of the observed spectral shifting lie in significantly decreased intermolecular interactions, which are particularly localized on the carbon chain. This is not surprising, as shorter chain fatty acids are dominated by hydrogen bonding interactions which are much stronger than intermolecular van der Waals forces that dominate the interactions for longer chain fatty acids. This finding proves the great potential for terahertz spectroscopy in understanding the origins of intermolecular interactions in condensed molecular systems, particularly for the characterization of the FFAs or in other practical settings.

In summary, we measured the fatty acids with even-number of carbon atoms from 12 carbons to 20 carbons using a THz-TDS system. The absorption coefficients were calculated. Several absorption bands were observed at room temperature between 0.5 to 2.75 THz. With the increase of the carbon chain length, these absorption bands shift towards lower frequencies indicating their association with the vibrational modes of the lattice. In the low temperature measurements, three absorption bands can be identified

that evolve to lower frequencies systematically with increasing carbon chain length. At 293 K, the peak locations show a linear dependence on the carbon chain length, which makes terahertz a potential tool for FFA characterization in practical settings. At 96 K, the spectra were further compared with those calculated by *ab initio* calculations. The calculation enabled the assignment of the experimental spectra, and revealed that the experimentally observed bands exhibit identical mode-types, which is uncommon in the terahertz spectral range. The similarities in mode types allows these materials to be one of the few where spectral shifting of terahertz phonons across different materials is acceptable, and provides a basis for directly extracting the intermolecular interaction strengths for the series of studied FFAs. The findings in this paper provides a means for the complete description of intermolecular interactions in fatty acids.

SF thanks the funding support from the National Natural Science Foundation of China (61805150) and the Shenzhen University Start-up Fund (00000148). MTR thanks the University of Vermont for its continued support. VPW and SF thank the the Australian Research Council for financial support (Discovery Project, DP 150100635 and Linkage Project LP 160100325). VPW is the recipient of the Cancer Council of Western Australia Youngberg's Fellowship.

References

1 A. Pappas, *Dermato-endocrinology,* 2009, ***1***, 72-76.
2 D. Khnykin, J. H. Miner, F. Jahnsen, *Dermato-endocrinology,* 2011, ***3***, 53-61.
3 S. J. Van, M. Janssens, E. C. Kaye, P. J. Caspers, A. P. Lavrijsen, R. J. Vreeken, J. A. Bouwstra, *Exp.Dermatol.,* 2014, ***23***, 45-52.
4 D. Senyilmaztiebe, D. H. Pfaff, S. Virtue, K. V. Schwarz, T. Fleming, S. Altamura, M. U. Muckenthaler, J. Okun, A. Vidalpuig, P. Nawroth, *Nature Communications,* 2018, ***9***, 3129.
5 J. Qin, Y. Ying, L. Xie, *Applied Spectroscopy Reviews,* 2013, ***48***, 439-457.
6 P. Somerharju, J. A. Virtanen, K. H. Cheng, *Biochimica et Biophysica Acta (BBA) - Molecular and Cell Biology of Lipids,* 1999, ***1440***, 32-48.
7 S. Sonnino, A. Prinetti, H. Nakayama, M. Yangida, H. Ogawa, K. Iwabuchi, *Glycoconj.J.,* 2009, ***26***, 615-621.
8 R. G. Sinclair, A. F. Mckay, R. N. Jones, *J.Am.Chem.Soc.,* 1952, ***74***, 2570-2575.
9 R. N. Jones, A. F. Mckay, R. G. Sinclair, *J.Am.Chem.Soc.,* 2002, ***74***, 2575-2578.
10 J. R. Beattie, S. E. J. Bell, C. Borgaard, A. Fearon, B. W. Moss, *Lipids,* 2006, ***41***, 287.
11 C. H. Warren, D. L. Hooper, *Canadian Journal of Chemistry,* 2011, ***51***, 3901-3904.
12 P. F. Taday, I. V. Bradley, D. D. Arnone, M. Pepper, *J.Pharm.Sci.,* 2003, ***92***, 831-838.
13 J. A. Zeitler, D. A. Newnham, P. F. Taday, T. L. Threlfall, R. W. Lancaster, R. W. Berg, C. J. Strachan, M. Pepper, K. C. Gordon, T. Rades, *J.Pharm.Sci.,* 2010, ***95***, 2486-2498.
14 Strachan, J. Clare, Rades, Thomas, Newnham, A. David, Gordon, C. Keith, Michael, *Chemical Physics Letters,* 2004, ***390***, 20-24.
15 B. Born, S. J. Kim, S. Ebbinghaus, M. Gruebele, M. Havenith, *Faraday Discuss.,* 2008, ***141***, 161-173.
16 U. Heugen, G. Schwaab, E. Bründermann, M. Heyden, X. Yu, D. M. Leitner, M. Havenith, *Proc.Natl.Acad.Sci.U.S.A.,* 2006, ***103***, 12301-12306.
17 M. T. Ruggiero, W. Zhang, A. D. Bond, D. M. Mittleman, J. A. Zeitler, *Phys.Rev.Lett.,* 2018, ***120***, 196002.
18 M. T. Ruggiero, J. Kölbel, L. Qi, J. A. Zeitler, *Faraday Discuss.,* 2018, 10.1039.C8FD00042E.
19 J. Neu, H. Nikonow, C. A. Schmuttenmaer, *The Journal of Physical Chemistry A,* 2018, ***122***, acs.jpca.8b04978.
20 J. T. Jr, T. M. Korter, *Journal of Physical Chemistry A,* 2013, ***117***, 10504-10512.
21 C. S. P. Jr, O. Kambara, S. Kawaguchi, K. Yamamoto, K. Tominaga, *Journal of Infrared Millimeter & Terahertz Waves,* 2010, ***31***, 799-809.
22 B. M. Fischer, M. Walther ., P. Jepsen U., *Physics in Medicine & Biology,* 2002, *47,* 3807-3814.
23 M. D. King, W. D. Buchanan, T. M. Korter, *J.Pharm.Sci.,* 2011, ***100***, 1116-1129.
24 R. Dovesi, A. Erba, R. Orlando, C. M. Zicovich-Wilson, B. Civalleri, L. Maschio, M. Rérat, S. Casassa, J. Baima, S. Salustro, *Wiley Interdisciplinary Reviews Computational Molecular Science,* 2018, ***8***, e1360.
25 R. Krishnan, J. S. Binkley, R. Seeger, J. A. Pople, *J.Chem.Phys.,* 1980, *72,* 650-654.
26 J. P. Perdew, K. Burke, M. Ernzerhof, *Phys.Rev.Lett.,* 1996, ***77***, 3865-3868.
27 G. Stefan, A. Jens, E. Stephan, K. Helge, *J.Chem.Phys.,* 2010, ***132***, 154104.
28 S. Grimme, S. Ehrlich, L. Goerigk, *Journal of Computational Chemistry,* 2011, ***32***, 1456-1465.
29 Y. Noel, C. Zicovich-Wilson, B. Civalleri, P. D'Arco, R. Dovesi, *Physical Review B,* 2001, ***65***, 014111.
30 F. Pascale ., C. Zicovich-Wilson, F. Gejo Ló, B. Civalleri ., R. Orlando ., R. Dovesi ., *Journal of Computational Chemistry,* 2004, ***25***, 888–897.
31 C. Zicovich-Wilson, F. Pascale ., C. Roetti ., V. R. Saunders, R. Orlando ., R. Dovesi ., *Journal of Computational Chemistry,* 2004, ***25***, 1873-1881.